Numerical Study of the Flow Field and Heat Transfer of a Non-Newtonian Magnetic Nanofluid in A Vertical Channel Affected by A Magnetic Field

Amireh Nourbakhsh*
Department of Mechanical Engineering,
University of Bu-Ali Sina, Hamedan, Iran
E-mail: nourbakhsh@basu.ac.ir
*Corresponding author

Amir Reza Sadeghi
Department of Mechanical Engineering,
University of Bu-Ali Sina, Hamedan, Iran
E-mail: ar.sadeghi1374@gmail.com

Received: 1 September 2021, Revised: 4 December 2021, Accepted: 5 January 2022

Abstract: The present paper examines thermal and hydrodynamic behavior of the incompressible laminar flow of a non-Newtonian magnetic nanofluid in a vertical rectangular channel numerically using two-phase mixture model, Carreau model, and finite volume method. The non-uniform transverse magnetic field is created by an electric current-carrying wire located along the channel. The Schiller-Naumann model is employed to calculate the slip velocity between the solid and liquid phases. The flow pattern and nanofluid temperature is assessed by changing effective parameters such as Reynolds number, the magnetic field strength, flow rate, mean axial temperature, and channel heat transfer. It is observed that the transverse secondary flow increases by increasing the magnetic strength due to Kelvin force. The hot fluid is transferred more from the sidewall to the center of the channel and the cold fluid moves from the center of the channel towards the wall, leading to an increase in heat transfer. Also, at low Reynolds numbers, more fluctuations occur in the velocity profile due to the dominance of Kelvin force over inertial force.

Keywords: Ferrofluid, Non-Newtonian Fluid, Magnetic Field Strength, Mixture Two-Phase Model, Reynolds Number

How to cite this paper: Amireh Nourbakhsh, and Amirreza Sadeghi "Numerical Study of the Flow Field and Heat Transfer of a Non-Newtonian Magnetic Nanofluid in A Vertical Channel Affected by A Magnetic Field", Int J of Advanced Design and Manufacturing Technology, Vol. 15/No. 2, 2022, pp. 105-118. DOI: 10.30495/admt.2022.1939334.1312.

Biographical notes: Amireh Nourbakhsh received his Ph.D. in Mechanical Engineering from Isfahan University of technology in 2010. She is currently assistant professor at the department of Mechanical Engineering, Bu Ali Sina University, Hamedan, Iran. Her current research interest includes computational fluid dynamics (CFD) and multiphase flows. She has published several journal papers in these fields and presented some conference articles in conferences. **Amir Reza Sadeghi** received his B.Sc. in Mechanical Engineering from Kermanshah University of technology in 2019 and at present he is a M.Sc. student at Bu Ali Sina University.

1 INTRODUCTION

The magnetic field affects different types of fluid flows. The study of flows under a magnetic field is called magnetohydrodynamics (MHD). MHD has different applications such as drug delivery, cell separation, fluid mixing, etc. [1-2]. Many investigators have employed MHD to intensify heat transfer rate in horizontal and vertical enclosures. For instance, Oreper and Szekely [3] investigated the effect of a magnetic field on the flow and thermal fields in a cavity with fixed temperature sidewalls. They showed that in this system, the strength of the magnetic field is an important factor in weakening the heat transfer (the higher the field strength, the lower the heat transfer). Grosan et al. [4] investigated the effect of magnetic field on free convection heat transfer in a porous closed cavity. They found that the magnetic field applied in the horizontal direction was more effective in preventing heat transfer than the magnetic field applied in the vertical direction.

Pak and Cho [5] for the first time investigated the heat transfer of a nanofluid in a tube experimentally. They studied the heat transfer of $Al_2O_3\gamma$/water nanofluid with a nanoparticles diameter of 13 nm and titanium oxide/water nanofluid with a particle diameter of 27 nm in the turbulent flow regime and showed that the heat transfer of Al_2O_3 γ /water nanofluid is higher than TiO_2/water nanofluid. They also provided a correlation for the Nusselt number of nanofluid. Li and Xuan [6] investigated the effect of CuO and Al_2O_3 nanoparticles with different diameters on different base fluids. They examined four different types of nanofluids, including copper oxide in water, copper oxide in ethylene glycol (EG), aluminum oxide in water, and aluminum oxide in EG. They showed that nanofluids have a higher conductivity than their base fluids and CuO nanoparticles. Compared to Al_2O_3 nanoparticles, Al_2O_3 ones lead to higher thermal conductivity. Chen et al. [7] investigated titanium oxide nanotubes with a diameter of 10 and a length of 100 nm. The water-based fluid and the laminar flow in the tube were under constant heat flux. Their results showed that the local heat transfer coefficient decreases in the longitudinal direction and reaches a constant value of 800 at Reynolds number of 1700. Also, no significant change in this value was observed for different volume fractions (0.5%, 1%, and 2.5%).

Khanafer et al. [8] for the first time simulated nanofluid flow numerically. They studied the natural convective flow of a mixture of water and copper in a square cavity and found that the heat transfer and velocity of the nanofluid relative to the pure fluid are increased due to the increase in thermal conductivity and the turbulent motion of the nanoparticles. Maiga et al. [9] numerically investigated the forced convection of laminar and turbulent nanofluid flow in a tube with constant heat flux. They used the single-phase model and considered the effect of nanoparticles only by placing the effect of nanofluid properties in the governing equations. Considering the mixture of water aluminum oxide and ethylene glycol aluminum oxide, they concluded that the shear stress and heat transfer increase with increasing the volume fraction of nanoparticles. Aluminum oxide/ethylene glycol nanofluid shows higher heat transfer for the same volume fraction and Reynolds number. Using the Lattice-Boltzmann method, Xuan et al. [10] numerically studied the heat transfer of a magnetic nanofluid in the presence of magnetic fields within a microchannel. In an experimental study, Lajvardi et al. [11] investigated the forced convection heat transfer of magnetic water-iron oxide nanofluid in a straight tube under constant wall heat flux and uniform magnetic field, in the direction of flow for laminar flow regime. Hojjat et al. [12] experimentally investigated the laminar heat transfer of a non-Newtonian nanofluid in a circular tube with constant wall temperatures. They showed that the addition of nanoparticles increases the heat transfer coefficient of the base fluid and this increase is proportional to the increase in the volume fraction of nanoparticles and the Peclet number. They also obtained these results for the turbulent flow [13]. Farooq et al. [14] investigated the natural convection of a non-Newtonian nanofluid in a U-shaped cavity under a magnetic field. They showed the effect of the magnetic field angle on Nu_{ave}, where Nu_{ave} reaches its maximum value at an angle of 30°. Wang and Lei [15] investigated the effect of the magnetic hydrodynamic flow of liquid metal and its heat transfer in a rectangular channel containing microchannels. They found that the effect of this flow intensifies with the increase of the magnetic field. The increase of the heat transfer was due to the jet flow on the wall caused by the magnetic field. Their results also showed that Nu_{ave} increases with the Hartmann number, indicating that the magnetic field is useful for increasing heat transfer. Salimefendigil and Oztop [16] investigated the effect of forced convection for CuO-water nanofluid in a circular cylinder and found that the wake area of the cylinder is affected by the magnetic field and the average heat transfer changes by the Reynolds number. Izadi et al. [17] studied natural convection heat transfer of a magnetic nanofluid in the presence of porous medium under the influence of variable magnetic fields for the magnetic numbers of 100-5000, Hartmann numbers of 0-50, and porosity coefficients of 0.1-0.9. They found that for a given Reynolds number, the Nusselt number is enhanced with the magnetic number. Abdelraheem et al. [18] evaluated the impact of magnetic field on nanofluid flow in a square cavity containing four fins and an inner obstacle. It was revealed that as the Hartmann number is increased, the solid and fluid particles are blended more. Aboud et al. [19] considered the heat transfer and

hydrodynamics of Cu/water non-Newtonian nanofluid flow inside annulus cavity under the effect of a magnetic field for Prandtl number of 6.2, Grashof number of 100, Richardson numbers of 0-1, and Hartmann numbers of 0-60. The outer rotating cylinder was at a cold temperature and the inner stationary one was at a hot temperature. It was revealed that the Nusselt number is enhanced with the Richardson number and the flow pattern affected by the magnetic field significantly. Kumar et al. [20] analyzed the influence of axisymmetric magnetic field strength on the thermal behavior of a ferrofluid and demonstrated that self-induced magnetic field plays a vital role in the cooling process of a wire with electric current. Zheng et al. [21] evaluated the effect of magnetic field on the hydrodynamic and thermal performance of a plate heat exchanger saturated with ferrofluids containing spherical particles of Fe_3O_4. It was demonstrated that magnetic particles deposition affects the thermal performance of the heat exchanger and changes the flow characteristics. Rawa et al. [22] evaluated the effect of blade angle on thermal-hydraulic efficiency of non-Newtonian nanofluid flow in a helical channel under the influence of a magnetic field using the Eulerian-Eulerian Two-Phase approach. They revealed that maximum performance can be achieved for the blade angle of 60.

In the present work, the thermal and hydrodynamic behavior of the laminar incompressible flow of a magnetic non-Newtonian nanofluid (assuming a non-Newtonian base fluid with 4% iron oxide) in a vertical rectangular channel in the presence of different magnetic fields is investigated. One of the innovations of the present work is to examine the impact of non-Newtonian fluid and magnetic field on heat transfer rate simultaneously. The Schiller-Naumann model is used to calculate the slip velocity between the solid and liquid phases. The flow and temperature patterns of the nanofluid with the non-Newtonian base fluid will be investigated and the rate of change in the flow pattern, average axial temperature, and channel heat transfer will be analyzed by changing the Reynolds number and the magnetic field strength.

2 EQUATIONS, NUMBERS, SYMBOLS, AND ABBREVIATIONS

In the present simulations, the Carreau non-Newtonian model is used to model the non-Newtonian behavior of the fluid flow. This model uses the following equation to calculate the viscosity [23-24]:

$$\frac{\eta-\eta_\infty}{\eta_0-\eta_\infty}=(1+(\lambda\gamma)^2)^{\frac{n-1}{2}} \quad (1)$$

Where, λ is a time constant, n is the non-Newtonian fluid power index, η_0 is the viscosity at zero shear rate and η_∞ is the viscosity at an infinite shear rate. When $\gamma >> \frac{1}{\lambda}$, the Carreau model fluid acts like a Newtonian fluid, and when the shear rate is maximum ($\gamma << \frac{1}{\lambda}$), the Carreau model fluid acts like the power-law fluid.

The mixed model is used to simulate two-phase fluid. The mass, momentum, and energy conversion equations for the mixture are expressed by the following equations:

$$\nabla.(\rho_m \cdot \vec{v}_m)=0 \quad (2)$$

$$\nabla.(\rho_m\vec{v}_m\vec{v}_m)=-\nabla P_m+\nabla.(\mu_m\nabla\vec{v}_m)+\nabla.(\alpha_p\rho_p\vec{v}_{dr\cdot p}\vec{v}_{dr\cdot p})+\mu(\vec{M}\cdot\nabla)\vec{H} \quad (3)$$

$$\nabla\cdot[(\alpha_p\rho_p c_{p\cdot p}\vec{v}_p)+(1-\alpha_p)\rho_f c_{p\cdot f}\vec{v}_f)T]=\nabla\cdot(k_m\nabla T) \quad (4)$$

Where, ρ_m, μ_m, and k_m are the mixture density, mixture viscosity, and thermal conductivity of the mixture, respectively, and α_p is the volume percentage of magnetic particles, which in the present work is considered to be 4%. The last term of the right side of the momentum equation is related to the Kelvin volume force due to the magnetic field:

$$\nabla.(\alpha_p\rho_p\vec{v}_m)=-\nabla.(\alpha_p\rho_p\vec{v}_{dr\cdot p}) \quad (5)$$

The volume percentage equation is derived from the continuity equation for the second phase, in which the subtitle p refers to the second phase or magnetic particles:

$$\vec{v}_m=\frac{\alpha_p\rho_p\vec{v}_p+(1-\alpha_p)\rho_f\vec{v}_f}{\rho_m} \quad (6)$$

Where, $\vec{v}_{dr\cdot p}$ is drift velocity which is related to the slip velocity $\vec{v}_{pf}$ [25]:

$$\vec{v}_{dr\cdot p}=\vec{v}_{pf}-\frac{\alpha_p\rho_p}{\rho_m}(\vec{v}_f-\nu_p) \quad (7)$$

$$\vec{v}_{pf}=(\vec{v}_p-\vec{v}_f) \quad (8)$$

Since the force acting on different phases is different, different phases have a relative velocity or slip velocity relative to each other. The slip velocity caused by magnetic forces is calculated by the following equations:

$$\sum F_p=0 \rightarrow \mu\cdot m_p L(\xi)\nabla\vec{H}-3\Pi\mu_f d_p\vec{v}_{pf}=0 \quad (9)$$

$$\vec{v}_{pf}=\frac{\mu\cdot m_p L(\xi)}{3_\Pi\mu_f d_p}\nabla\vec{H} \quad (10)$$

To obtain the properties of the mixture, the volume properties of the phases are averaged, which is expressed by the following equation:

$$\phi_m = \alpha\phi_p + (1-\alpha)\phi_f \quad (11)$$

The dimensionless number is expressed as follows:
Magnetic number:

$$Mn = \frac{\mu \cdot H_{max}^2 h^2}{\rho_m \alpha_m^2} \quad (12)$$

3 PROBLEM DEFINITION AND NUMERICAL MODELING

The thermal and hydrodynamic behaviour of the laminar and incompressible flow of a magnetic non-Newtonian nanofluid (assuming a non-Newtonian base fluid with 4% iron oxide) in a vertical rectangular channel in the presence of a magnetic field is investigated. This non-uniform transverse magnetic field is created by an electric current-carrying wire located along the channel. The geometry of the channel with a square cross section is drawn in Design Modeler software. The channel is considered vertical with dimensions of 20×2×2 cm. Figure 1 shows a schematic of the channel in this software.

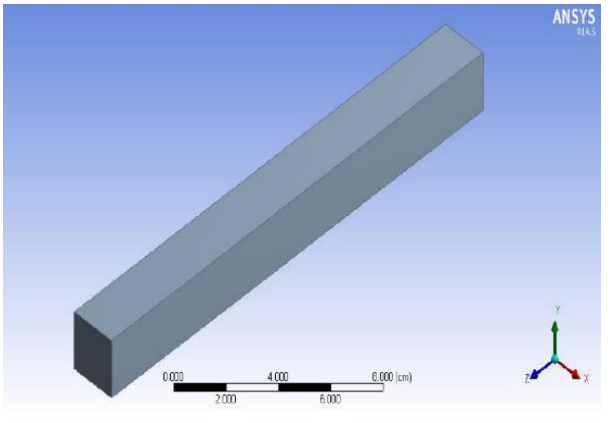

Fig. 1 A schematic of the channel in Design Modeler software.

As shown in "Fig. 2", the mesh contains structured grids. Near the walls, where the variables change more and the simulation is more important, a finer grid is used. The naming of the channel walls is shown in "Fig. 3". The wall next to the wire is considered wall 1 and the channel walls are counted clockwise.
After the computational grid is generated using ANSYS Meshing software, it is imported into FLUENT software. The simulations are performed in three dimensions and steadily, and a pressure-based solver is used due to the nature of the problem. For calculations, a mixture multiphase model is used. In addition, the slip velocity is activated in the software to consider the slip effects between the solid phase and the fluid phase, and a subroutine is written for the slip velocity considering the magnetic force due to the non-uniform transverse magnetic field [26-27].

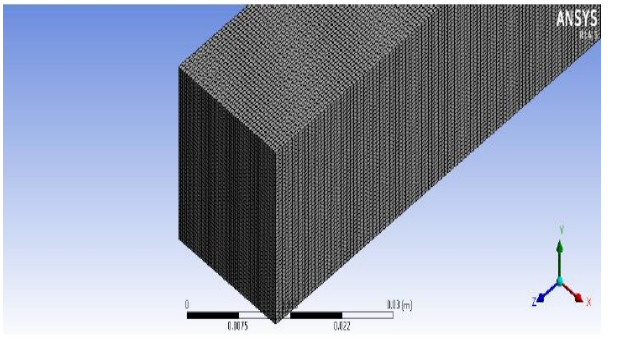

Fig. 2 Structured computational grid for the channel.

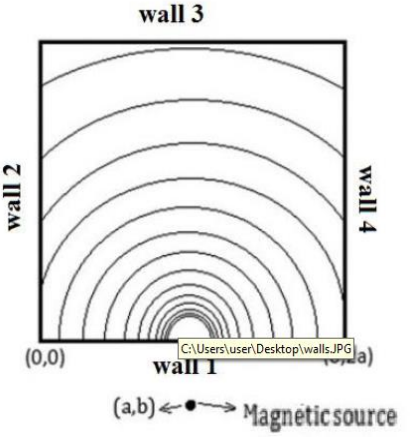

Fig. 3 The naming of the channel walls.

The nanofluid used is a mixture of non-Newtonian fluid water and Fe_3O_4 particles. The properties of fluids and particles are given in "Table 1".

Table 1 Properties of fluid, nanoparticles, and ferrofluid

Properties	Fluid	Nanoparticles	Ferrofluid
Density, kg/m^3	1024	5200	1191
Specific heat capacity, J/kg.K	4001.1	670	3419.36
Thermal conductivity, W/mK	0.596	6	0.6514

Since the fluid is non-Newtonian, the non-Newtonian fluid model must be determined, as well as parameters such as time constant, power-law index, zero shear rate viscosity, and infinite shear rate viscosity. Properties of

non-Newtonian fluids and the parameters of the Carreau non-Newtonian model are given in "Table 2". Non-Newtonian fluid is selected as the first phase and Fe_3O_4 particles as the secondary phase. The effects of the phases on each other, such as drag force, must be determined. In the simulations, the Schiller-Naumann model is used to determine the drag coefficient of particles.

Table 2 Properties of non-Newtonian fluid and parameters of Carreau model

Case	Time constant λ	Power law index n	Zero shear viscosity (η_o)	Infinite shear viscosity (η_∞)
1	0.576	0.756	0.209	0.00249

The inlet velocity boundary condition is used for the inlet and the pressure output one is used for the channel outlet. For walls, the boundary condition is no slip. The inlet velocity varies according to the Reynolds number, for example for the Reynolds number 50, the inlet velocity is assumed to be 0.0025 m/s. The fluid inlet temperature is 300 K. All walls are considered at a constant temperature of 370 K. The fluid begins to heat up as it enters the channel. The outlet pressure of the channel is assumed to be atmospheric pressure and the temperature of the reverse flow is assumed to be 370 K.

4 RESULTS AND DISCUSSION

4.1. Grid Independence and Validation

First, the independence of the results from the computational grid is examined. Figure 4 shows the wall Nusselt number changes along the channel for the three computational grids of 21×21×100, 46×46×300, and 51×51×400 at the Reynolds number of 50 and the magnetic field strength zero. As can be seen, by increasing the grid points from 46×46×300 to 51×51×400, there is no significant change in the Nusselt number. As a result, in order to reduce the cost and time of calculations, the 46×46×300 computational grid is used. To validate the results, simulations of Aminfar et al. [28] are used. They investigated the effect of a transverse magnetic field on the flow field and heat transfer of Newtonian nanofluids. Therefore, it is considered that the fluid is as Newtonian at Reynolds number 50 and $Mn = 8.5 \times 10^2$. Figure 5 shows the velocity profiles at the cross-section of x/a = 1 and z/a = 10. It can be seen that the results are in good agreement with the reference results.

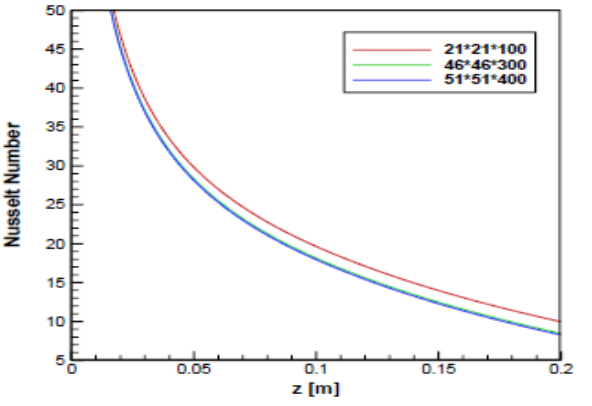

Fig. 4 Nusselt number along the channel for three computational grids at Reynolds number of 50 and zero magnetic field strength.

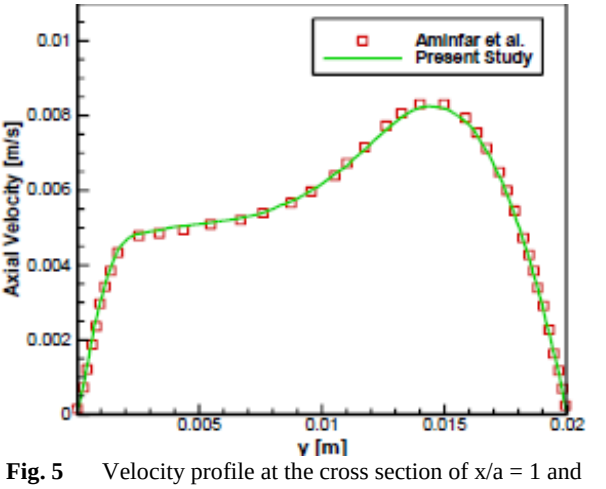

Fig. 5 Velocity profile at the cross section of x/a = 1 and z/a = 10.

4.2. Results

In this section, the results obtained from the simulations of non-Newtonian nanofluid are presented.

4.2.1. Effect of Non-Uniform Transverse Magnetic Field on Flow Pattern and Heat Transfer

In this section, the effect of increasing the magnetic field strength on the vertical velocity profile, temperature distribution in the middle sections of the channel, streamlines, and temperature changes in the direction of the channel is investigated. One of the methods to increase the strength of the magnetic field is to increase the intensity of the electric current passing through the wire that produces the magnetic field. By changing the intensity of the electric current, four magnetic fields with Mn = 0, 1.0×10^8, 1.17×10^8, and 1.34×10^8. Figure 6 shows the effects of increasing the magnetic field strength on the dimensionless profile of the axial velocity at z/a=10. It is observed that the axial velocity is pushed more towards the channel wall.

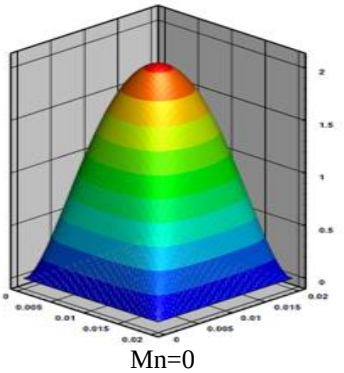

Mn=0

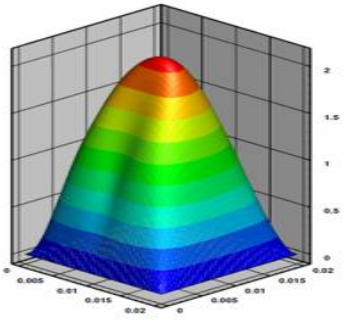

Mn=1 × 10^8

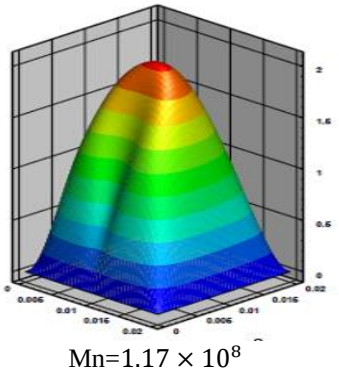

Mn=1.17 × 10^8

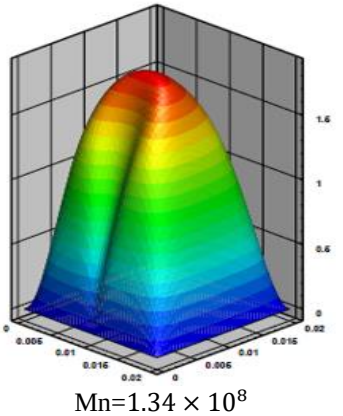

Mn=1.34 × 10^8

Fig. 6 Three-dimensional profile of dimensionless axial velocity with inlet velocity at cross section z/a = 10 for different magnetic field strengths and Reynolds number of 50.

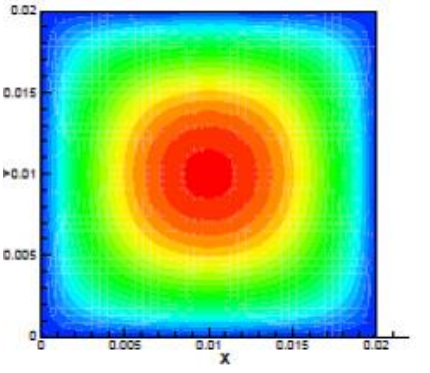

Mn=0

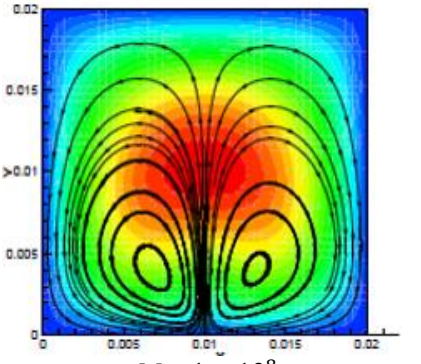

Mn=1 × 10^8

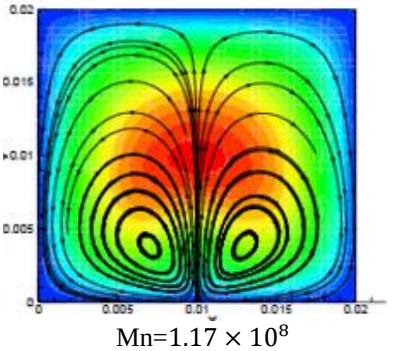

Mn=1.17 × 10^8

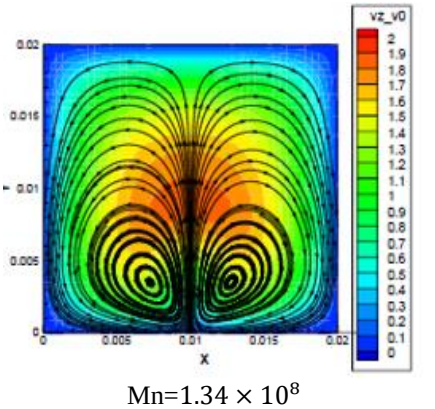

Mn=1.34 × 10^8

Fig. 7 Streamlines and the axial velocity contour at cross section z/a = 10 for different magnetic field strengths and Reynolds number of 50.

In "Fig. 7", the streamlines and the axial velocity contour at the cross-sectional area z/a = 10 are plotted for Mn = 0, 1.0×10^8, 1.17×10^8, and 1.34×10^8 and the Reynolds number of 50. As the strength of the magnetic field increases, the density of the streamlines and secondary flow strength are enhanced. Also, the center of the vortex is transmitted to the current-carrying wire and a stronger vortex is created.

Figure 8 shows the effect of increasing the strength of the magnetic field on the axial velocity profile at the cross section of z/a = 10 and x/a = 1. As can be seen, the curvature of the left side of the velocity profile increases with increasing the magnetic field strength compared to the case with no magnetic field.

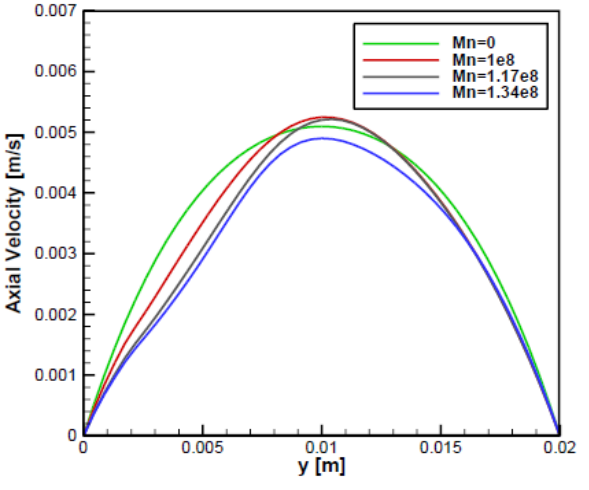

Fig. 8 Vertical velocity profile at the cross section of z/a = 10 and x/a = 1 for different magnetic field strengths at Reynolds number of 50.

Changes in the fluid flow pattern cause variations in the temperature pattern and heat transfer of the fluid. For this purpose, the fluid temperature contour at the cross-sectional area, z/a = 10, is shown in "Fig. 9". As the non-uniform transverse magnetic field increases, the transverse secondary flow increases due to Kelvin force and hot fluid is transferred with more intensity from the side of the wall to the center and cold fluid is transferred from the center to the lower wall, leading to an increase in the heat transfer.

Figure 10 shows the fluid temperature contours at the cross section x/a = 1 for four different magnetic field strengths. As expected, with increasing magnetic field strength, most of the channel is occupied by hot fluid and on the other hand, the flow pattern changes in such a way that at each axial section, there is no difference between the temperature changes in the center and in the vicinity of the wall. It is just a function of the distance from the channel inlet.

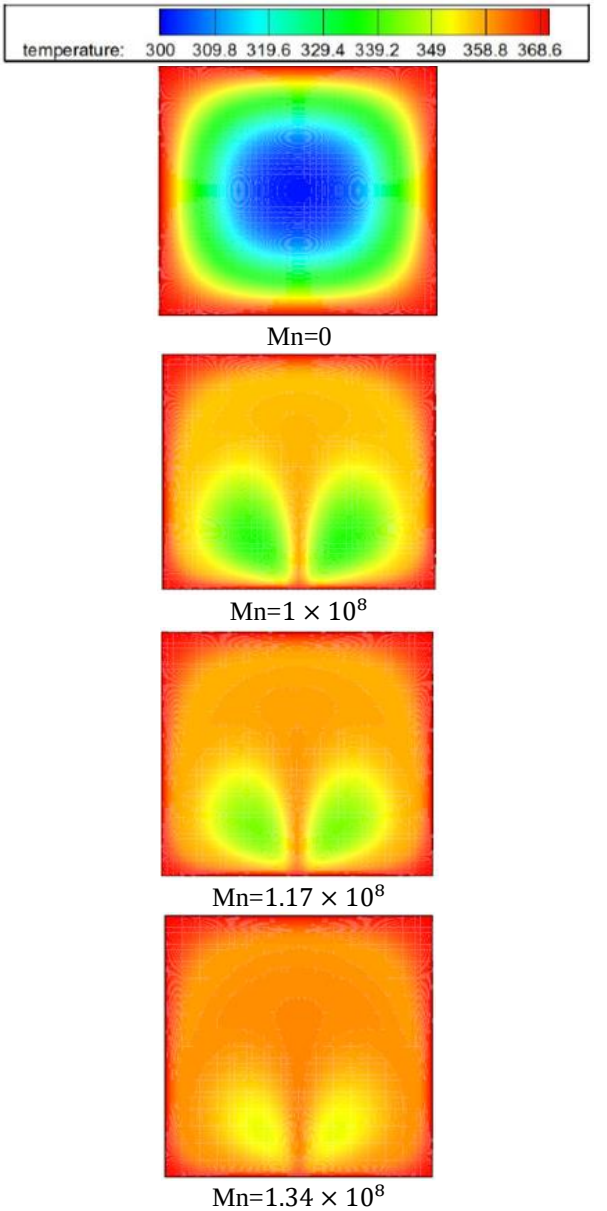

Fig. 9 Fluid temperature contours for different magnetic field strengths at cross section z/a = 10 at Reynolds number of 50.

In order to investigate the effects of increasing the strength of the magnetic field on the total heat transfer from the walls, the amount of total heat transfer rate from each wall is calculated. The heat transfer rate of the walls is shown in "Fig. 11". In the absence of a magnetic field, the heat transfer from all walls is equal to 36.55 W. By applying a non-uniform transverse magnetic field, a secondary flow is formed in the channel, which causes the hot fluid to be transferred from the side of wall 1 upwards, resulting in a significant increase in the rate of heat transfer from this wall.

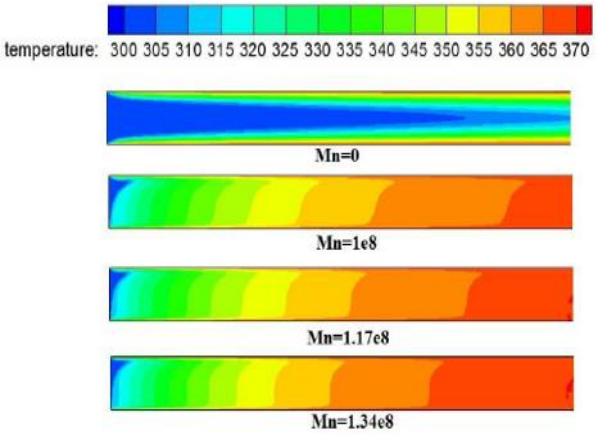

Fig. 10 Fluid temperature contours for different magnetic field strengths at cross section x/a = 1 at Reynolds number of 50.

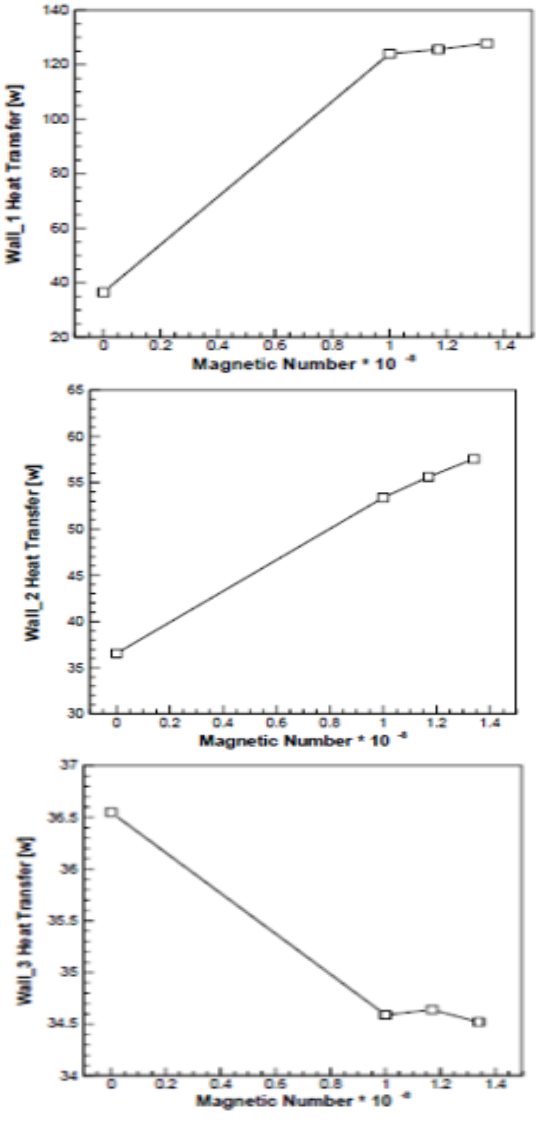

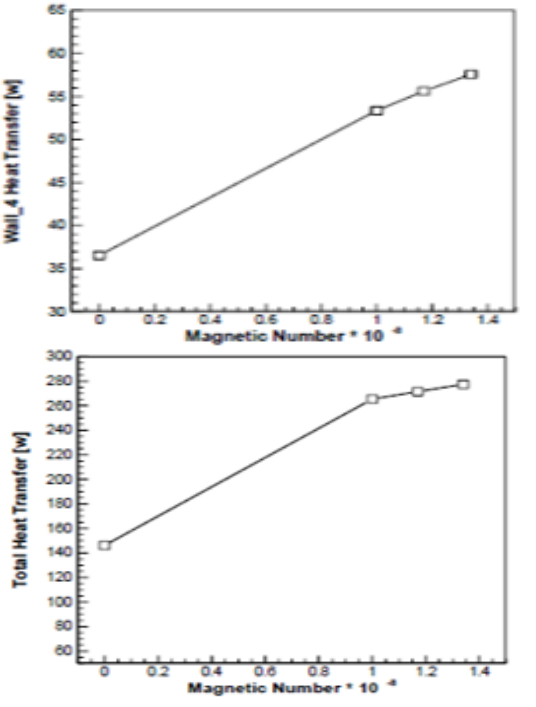

Fig. 11 Total heat transfer rate versus magnetic number calculated on channel walls for different magnetic field strengths at Reynolds number of 50.

On walls 2 and 4, which are located on the sides ("Fig. 3"), the amount of heat transfer is increased, but the amount of this increase is not as much as the increases in heat transfer in wall 1. In the case of wall 3, the heat transfer pattern is slightly different and is reduced by 2 W by applying a magnetic field. The reason for a reduction in heat transfer is the motion of hot fluid from wall 1 towards wall 3.

4.2.2. Effect of Reynolds Number on Flow Pattern and Heat Transfer

In this section, the effect of Reynolds number on the heat transfer rate of nanofluid exposed to a transverse non-uniform magnetic field generated from a current-carrying wire is investigated. Fluid flow with Reynolds numbers 25, 50, 100, and 200 is considered. To increase the Reynolds number, the flow velocity at the channel inlet is increased. The nanofluid velocities for the Reynolds numbers 25, 50, 100, and 200 are 0.00125, 0.0025, 0.005, and 0.01 m/s, respectively.

First, the three-dimensional axial velocity profile of the nanofluid is investigated. Figure 12 shows the axial velocity profile of the ferrofluid. At each Reynolds number, the axial velocity is dimensionless with the fluid inlet velocity. As shown in "Fig. 12", the velocity profile at lower Reynolds numbers has a higher maximum; but as the Reynolds number increases, the velocity profile becomes more uniform.

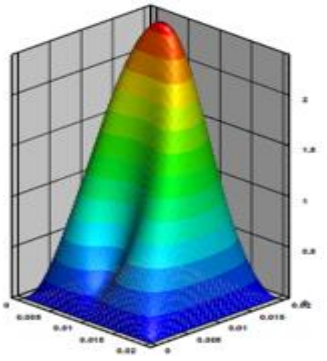

Re=25

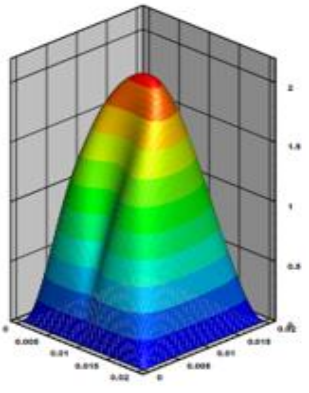

Re=50

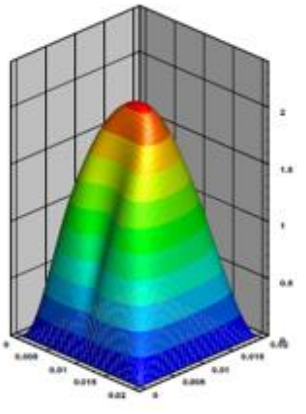

Re=100

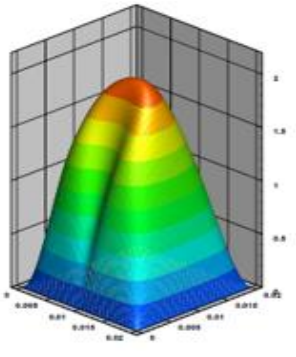

Re=200

Fig. 12 Non-dimensional profile of axial velocity on plane z/a = 10 for Reynolds numbers 25, 50, 100, and 200 and magnetic field strength of 1.17×10^8.

Figure 13 shows the streamlines and velocity contours for plane z/a = 10. As can be seen at the Reynolds number of 25, the dimensionless velocity of the fluid in the central region of the channel is greater. As the velocity increases, the density of the streamlines decreases.

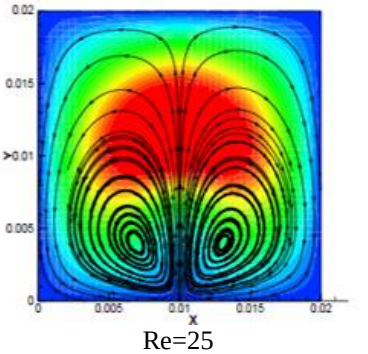

Re=25

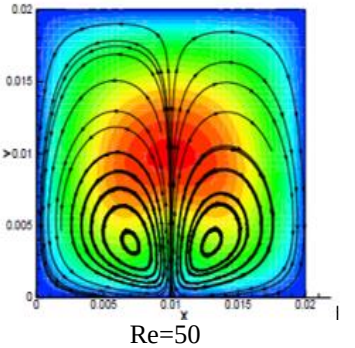

Re=50

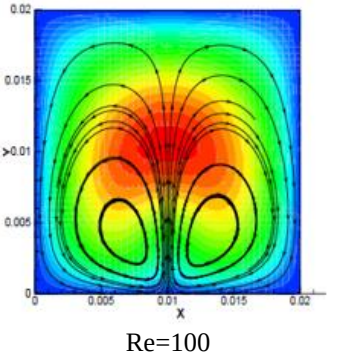

Re=100

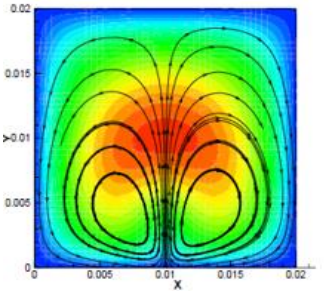

Re=200

Fig. 13 Streamlines and velocity contours on plane z/a = 10 for Reynolds numbers 25, 50, 100, and 200 and magnetic field strength of 1.17×10^8.

Figure 14 shows the effect of the Reynolds number on the axial velocity profile at the cross section of z/a = 10 and x/a = 1. As the Reynolds number decreases, the curvature to the left of the velocity profile decreases. This is due to the greater dominance of the Kelvin force over the inertial force at these Reynolds numbers, creating more distortion in the velocity profile.

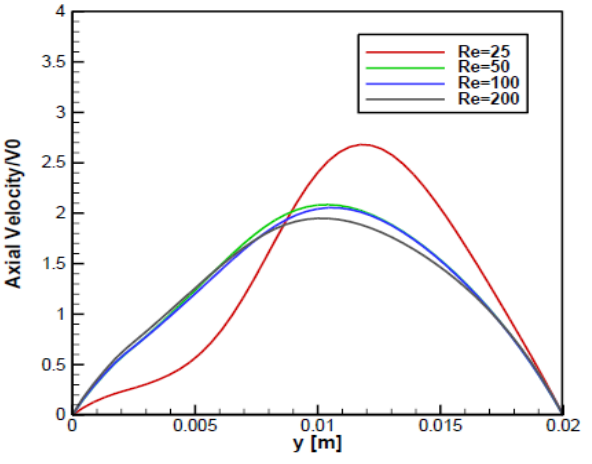

Fig. 14 Dimensionless axial velocity plane z/a = 10 and x/a=1 for Reynolds numbers 25, 50, 100, and 200 and magnetic field strength of 1.17×10^8.

Figure 15 shows the nanofluid temperature contours at z/a = 10, Reynolds numbers of 25, 50, 100, 200, and magnetic field strength of 1.17×10^8. At lower Reynolds numbers, the average fluid temperature is higher than the mean fluid temperature at higher Reynolds numbers. It may be expected that since the heat transfer rate is higher, the nanofluid temperature is higher at lower the Reynolds numbers. But it should be noted that the rate of heat transfer is higher at higher Reynolds numbers. These contours show the temperature of the fluid and do not give information about the rate of heat transfer.

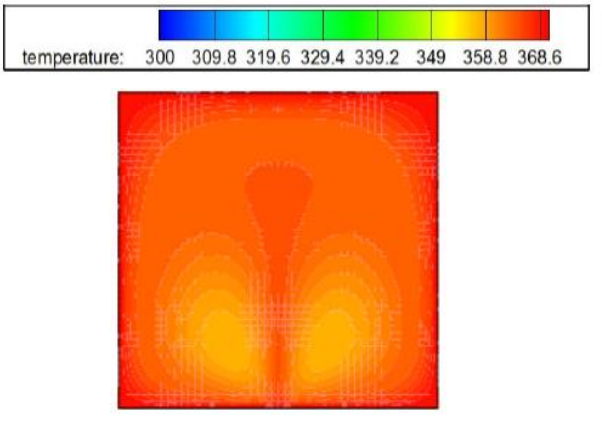

Re=25

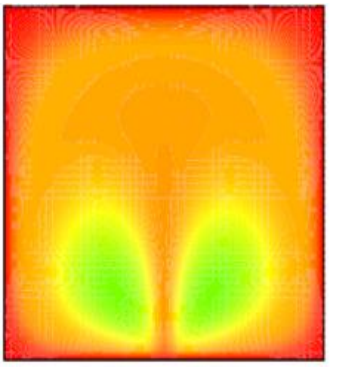

Re=50

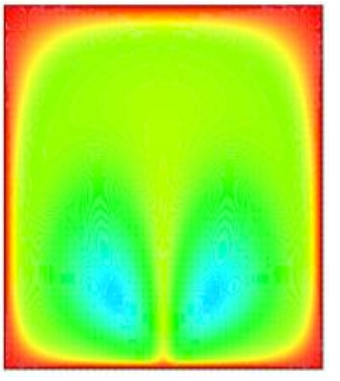

Re=100

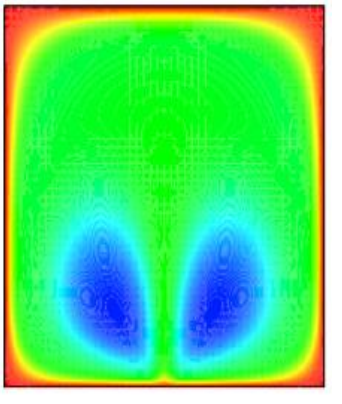

Re=200

Fig. 15 The nanofluid temperature contours at z/a = 10, Reynolds numbers of 25, 50, 100, 200, and magnetic field strength of 1.17×10^8.

The higher temperature at low Reynolds numbers is due to that the fluid stays in the channel longer due to its lower velocity and has more time to transfer heat. Based on the equation $q = h(T_{eq} - T_{wall})$, it should be noted that although T_{eq} is higher at lower Reynolds, the amount of h at higher Reynolds is so large that it compensates for this reduction. Therefore, at higher Reynolds, the rate of heat transfer increases.

Figure 16 shows the nanofluid temperature contours at x/a = 1 plane at Reynolds numbers of 25, 50, 100, 200 and magnetic field strength of 1.17×10^8. At lower Reynolds numbers, the fluid temperature reaches the surface temperature sooner. This is because, at lower Reynolds numbers, the fluid stays in the channel longer; therefore, the average channel temperature is lower at lower Reynolds numbers. Meanwhile, at lower Reynolds numbers, the temperature is uniform across the channel.

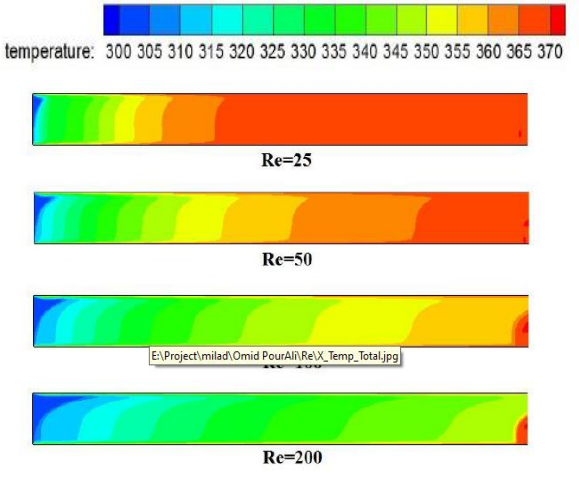

Fig. 16 The nanofluid temperature contours at x/a = 1, Reynolds numbers of 25, 50, 100, 200, and magnetic field strength of 1.17×10^8.

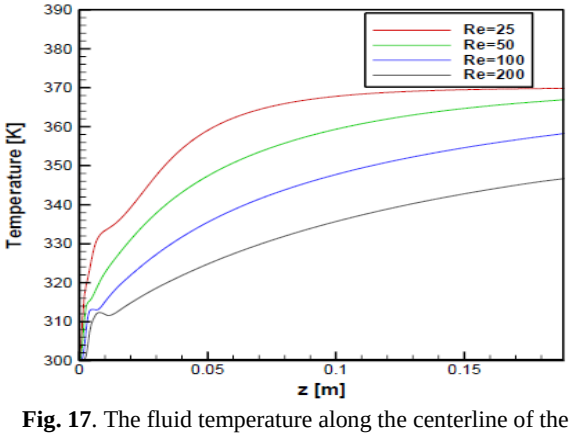

Fig. 17. The fluid temperature along the centerline of the channel for Reynolds numbers of 25, 50, 100, and 200 and magnetic field strength of 1.17×10^8.

Figure 17 shows the temperature of the nanofluid along the channel at its centerline. The temperature changes correspond to the results of "Fig. 16". The fluid remains in the channel longer and is exposed more to heat transfer at low Reynolds numbers, due to its lower velocity, and therefore has more opportunity to transfer heat. At Reynolds number of 25, for example, the flow of fluid through the half channel reaches approximately the temperature of the walls.

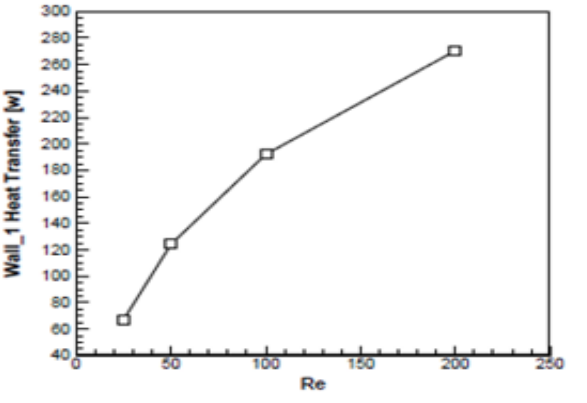

a

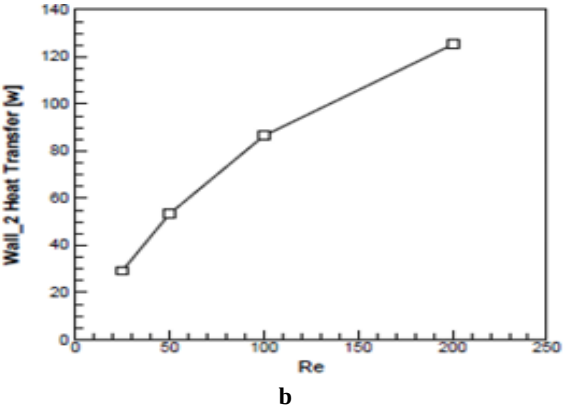

b

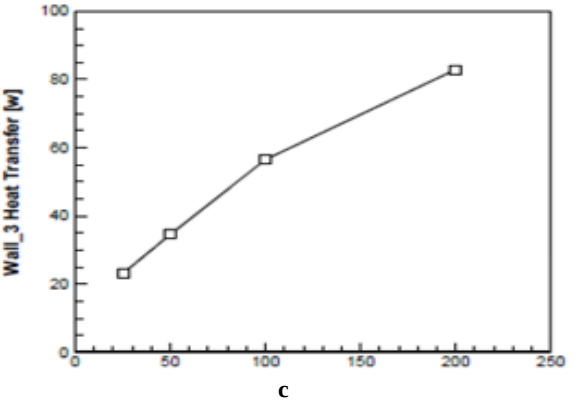

c

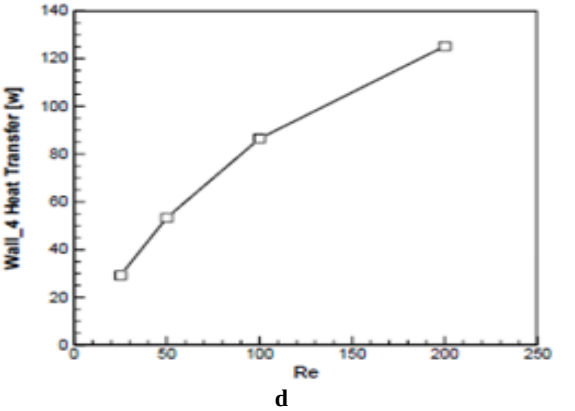

d

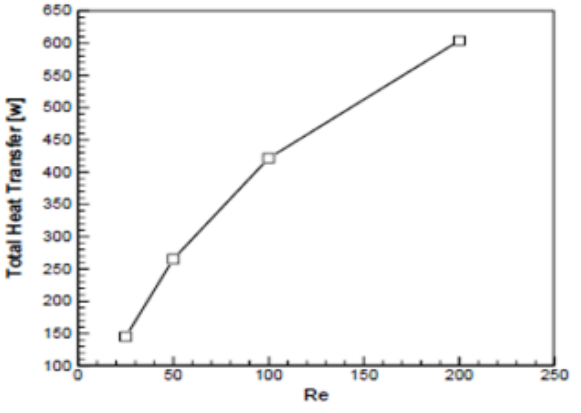

e

Fig. 18 Heat transfer in terms of Reynolds number for magnetic field strength of 1.17×10^8.

Figure 18 shows the rate of heat transfer from the channel walls and the total heat transfer for the Reynolds numbers of 25, 50, 100, and 200. By applying a non-uniform transverse magnetic field, a secondary flow is formed in the channel, which causes the hot fluid to be pushed from wall 1 upwards. Thus, a significant increase occurs in the heat transfer rate from this wall. In walls 2 and 4 (located on the sides), the rate of heat transfer is increased; however, this increase is not as much as the increase in heat transfer of wall 1.

Figure 18e demonstrates that the total heat transfer through the duct for different Reynolds numbers. As expected, as the Reynolds number increases, the heat transfer increases. This increase in heat transfer is due to the increase in fluid velocity and forced fluid convection. The increase in heat transfer has an almost linear relationship with the increase of Reynolds number. For example, by increasing the Reynolds number from 25 to 200, the total heat transfer rate has increased eightfold.

5 CONCLUSIONS

Heat transfer limitations and performance optimization of heat transfer systems have long been considered as constraints for engineering design. Recently, cooling efficiency has become a very important technical challenge and has limited the further development of various applications, such as military applications, electronic systems, and heat exchangers. One technique to increase heat transfer is to use magnetic nanofluids or ferrofluids. Ferrofluid is a mixture synthesized from a non-magnetic and non-conductive base fluid such as water and magnetized solid particles such as Fe_3O_4 with a diameter between 5 and 15 nm. Due to some properties, magnetic nanofluid behaves such a smart fluid. Since it is possible to control and operate the heat transfer process using an external magnetic field, the use of ferrofluid exposed to a magnetic field is an excellent solution.

In this paper, the flow field and heat transfer of a non-Newtonian magnetic nanofluid with Fe_3O_4 nanoparticles in a vertical channel with a square cross section exposed to a magnetic field were studied. This non-uniform transverse magnetic field was created by an electric current-carrying wire located along the channel. Effects of presence, magnetic field, and Reynolds number (flow velocity) on three-dimensional profiles perpendicular to the channel, two-dimensional axial velocity profile on the plate passing through the current-carrying wire, velocity contour and streamlines, temperature contours, temperature axial changes in channel centerline, and the amount of heat transfer of the whole channel were investigated.

The general results are as follows:

- The magnetic field exerts a force called the Kelvin force on the magnetic fluid.
- The magnetic force creates a transverse secondary flow and forms two vortices in the channel.
- The secondary flow pushes the hot fluid from the side of the wall to the center of the channel and moves the cold fluid from the center of the channel to the wall.
- The forced convective flow increases heat transfer and improves the performance of the heat exchanger.
- The amount of heat transferred from the channel is a function of the strength of the magnetic field.
- The amount of heat transfer is a function of the Reynolds number.
- At low Reynolds numbers, the Kelvin force overcomes the inertial force.
- In the absence of a magnetic field, heat transfer from all walls is equal.

REFERENCES

[1] Usefian, M., Bayareh, M., and Ahmadi Nadooshan, A., Rapid mixing of Newtonian and non-Newtonian Fluids in A Three-Dimensional Micro-Mixer Using Non-Uniform Field, Journal of Heat and Mass Transfer Research, Vol. 6, 2019, pp. 55-61.

[2] Shiriny, A., Bayareh, M., On Magnetophoretic Separation of Blood Cells Using Halbach Array of Magnets, Meccanica, Vol. 55, 2020, pp. 1903-1916, doi:10.1007/s11012-020-01225-y.

[3] Oreper, G. M., Szekely, J., The Effect of an Externally Imposed Magnetic Field On Buoyancy-Driven Flow in A Rectangular Cavity, Journal of Crystal Growth, Vol. 64, No. 3, 1983, pp. 505-515.

[4] Grosan, T., Revnic, C., Pop, I., and Ingham, D. B., Magnetic Field and Internal Heat Generation Effects On the Free Convection in A Rectangular Cavity Filled with A Porous Medium, International Journal of Heat and Mass Transfer, Vol. 52, No. 5-6, 2009, pp. 1525-1533.

[5] Pak, B. C., Cho, Y. I., Hydrodynamic and Heat Transfer Study of Dispersed Fluids with Submicron Metallic Oxide Particles, Experimental Heat Transfer, Vol. 11, No. 2, 1998, pp. 151-170.

[6] Li, Q., Xuan, Y., Convective Heat Transfer and Flow Characteristics of Cu-Water Nanofluid, Science in China Series E: Technolgical Science, Vol. 45, No. 5, 2002, pp. 408-416.

[7] Chen, H., Yang, W., He, Y., Ding, Y., Zhang, L., Tan, C., Lapkin, A., and Bavykin, D. V., Heat Transfer and Flow Behaviour of Aqueous Suspensions of Titanate Nanotubes (Nanofluids), Powder Technology, Vol. 183, No. 1, 2008, pp. 63-72.

[8] Khanafer, K., Vafai, K., and Lightstone, M., Buoyancy-Driven Heat Transfer Enhancement in A Two-Dimensional Enclosure Utilizing Nanofluids, International Journal of Heat and Mass Transfer, Vol. 46, No. 19, 2003, pp. 3639-3653.

[9] Maiga, S. E., Nguyen, C. T., Galanis, N., and Roy, G., Heat Transfer Behaviours of Nanofluids in A Uniformly Heated Tube, Superlattices and Microstructures, Vol. 35, No. 3-6, 2004, pp. 543-557.

[10] Xuan, Y., Li, Q., and Ye, M., Investigations of Convective Heat Transfer in Ferrofluid Microflows Using Lattice-Boltzmann Approach, International Journal of Thermal Sciences, Vol. 46, No. 2, 2007, pp. 105-111.

[11] Lajvardi, M., Rad, J. M., Hadi, I., Gavili, A., Isfahani, T. D., Zabihi, F., and Sabbaghzadeh, J., Experimental Investigation for Enhanced Ferrofluid Heat Transfer Under Magnetic Field Effect, Journal of Magnetism and Magnetic Materials, Vol. 322, No. 21, 2010, pp. 3508-3513.

[12] Hojjat, M., Etemad, S. G., Bagheri, R., and Thibault, J., Laminar Convective Heat Transfer of Non-Newtonian Nanofluids with Constant Wall Temperature, Heat and Mass Transfer, Vol. 47, 2011, pp. 203-209.

[13] Hojjat, M., Etemad, S. G., Bagheri, R., and Thibault, J., Turbulent Forced Convection Heat Transfer of Non-Newtonian Nanofluids, Experimental Thermal and Fluid Science, Vol. 35, No. 7, 2011, pp. 1351-1356.

[14] Farooq, H., Hamzah, H. K., Egab, K., Arici, M., and Shahsavar, M., Non-Newtonian Nanofluid Natural Convection in A U-Shaped Cavity Under Magnetic Field, International Journal of mechanical Sciences, Vol. 186, No. 15, 2020, pp. 105887.

[15] Wang, Z. H., Lei, T. Y., Liquid Metal MHD Effect and Heat Transfer Research in A Rectangular Duct with Micro – Channels Under a Magnetic Field, International Journal of Thermal Sciences, Vol. 155, 2020, pp. 106411.

[16] Selimefendigil, F., Öztop, H. F., Magnetic Field Effects On the Forced Convection of CuO-Water Nanofluid Flow in A Channel with Circular Cylinders and Thermal Predictions Using ANFIS, International Journal of Mechanical Sciences, Vol. 146-147, 2018, pp. 9-24.

[17] Izadi, M., Mohebbi, R., Amiri Delouei, A., and Sajjadi, H., Natural Convection of a Magnetizable Hybrid Nanofluid Inside a Porous Enclosure Subjected to Two Variable Magnetic Fields, International Journal of Mechanical Sciences, Vol. 151, 2019, pp. 154-169, https://doi.org/10.1016/j.ijmecsci.2018.11.019.

[18] Abdelraheem, M. A., Mohamed, E. M., and Alsedais, N., The Magnetic Field On a Nanofluid Flow Within a Finned Cavity Containing Solid Particles, Case Studies in Thermal Engineering, 25, 2021, pp. 100945, https://doi.org/10.1016/j.csite.2021.100945.

[19] Aboud, E. D., Rashid, H. K., Jassim, H. M., Ahmed, S. Y., Obaid Waheed Khafaji, S., Farooq, H. K., and Ali, H., MHD Effect On Mixed Convection of Annulus Circular Enclosure Filled with Non-Newtonian Nanofluid, Heliyon, Vol. 6, No. 4, 2020, pp. e03773, https://doi.org/10.1016/j.heliyon.2020.e03773.

[20] Kumar, V., Casel, M., Dau, V., and Woodfield, P., Effect of Axisymmetric Magnetic Field Strength On Heat Transfer from A Current-Carrying Micro-Wire in Ferrofluid, International Journal of Thermal Sciences, Vol. 167, 2021, pp. 106976, https://doi.org/10.1016/j.ijthermalsci.2021.106976.

[21] Zheng, D., Yang, J., Wang, J., Kabelac, S., and Sundén, B., Analyses of Thermal Performance and Pressure Drop in A Plate Heat Exchanger Filled with Ferrofluids Under a Magnetic Field, Fuel, Vol. 293, 2021, pp. 120432, https://doi.org/10.1016/j.fuel.2021.120432.

[22] Rawa, M. J. H., Abu-Hamdeh, N. H., Golmohammadzadeh, A., and Shahsavar Goldanlou, A., An Investigation On Effects of Blade Angle and Magnetic Field On Flow and Heat Transfer Of Non-Newtonian Nanofluids: a Numerical Simulation, International Communications in Heat and Mass Transfer, Vol. 120, 2021, pp. 105074, https://doi.org/10.1016/j.icheatmasstransfer.2020.105074.

[23] Masiri, S. M., Bayareh, M., and Nadooshan, A. A., Pairwise Interaction of Drops in Shear-Thinning Inelastic Fluids, Korea-Australia Rheology Journal, Vol. 31, No. 1, 2019, pp. 25–34, doi:10.1007/s13367-019-0003-8.

[24] Bayareh, M., Mortazavi, S., Effect of Density Ratio On the Hydrodynamic Interaction Between Two Drops in Simple Shear Flow, Iranian Journal of Science and Technology. Transactions of Mechanical Engineering, Vol. 35, 2011, pp. 121-132.

[25] Mohammadpourfard, M., Numerical Study of The Effects of Magnetic Fields On the Flow of Non-Newtonian Electrically Conductive Magnetized Nanofluid in A Vertical Channel, Journal of Modares Mechanical Engineering, Vol. 15, 2015, pp. 379-389 (in Persian).

[26] Bayareh, M., Mortazavi, S., Migration of a Drop In Simple Shear Flow at Finite Reynolds Numbers: Size and Viscosity Ratio Effects, Proceeding of International Conference on Mechanical, Industriel and Manufacturing Engineering (ICMIME), Cape Town, South Africa, 2010.

[27] Bayareh, M., Mortazavi, S., Equilibrium Position of a Buoyant Drop in Couette and Poiseuille Flows at Finite Reynolds Numbers. Journal of Mechanics, Vol. 29, No. 01, 2012, pp. 53–58, doi:10.1017/jmech.2012.109.

[28] Aminfar, H., Mohammadpourfard, M., and Kahnamouei, Y. N., A 3D Numerical Simulation of Mixed Convection of a Magnetic Nanofluid in The Presence of Non-Uniform Magnetic Field in A Vertical Tube Using Two Phase Mixture Model, Journal of Magnetism and Magnetic Materials, Vol. 323, No. 15, 2011, pp.1963-1972.